ISSN 0511-5728
The West Indian Journal of Engineering
Vol.43, No.2, January/February 2021, pp.4-11

Airflow and Heat Transfer Analysis within Flat-top Roofs Heated from Below

Ola Kamiyo

Department of Mechanical Engineering, University of Lagos, Lagos, Nigeria; Email: okamiyo@unilag.edu.ng;

(Received 29 April 2020; Revised 26 August 2020; Accepted 15 September 2020)

Abstract: *Natural convection in attic of non-conventional rooftops has received considerable attention in recent years due to its importance in thermal management of modern pitched-roof buildings. In this study, a finite-volume numerical investigation of laminar fluid dynamics and heat transfer of air within the attic of a flat-top roof structure has been predicted for bottom isothermal heating at varying pitch angle. The heat transfer between the walls results in multiple thermal plumes and multi-cellular flow structure with the number, size and strength of the counter-rotating cells reducing with increasing pitch angle. The results further show that the peculiar shape of the roof has significant effect on the fluid flow and heat transfer. Particularly, the truncated triangular architecture of the roof prevents the formation of large, dominating and upper-row cells at the midsection of the attic. At low pitch, the intensity of the vortices results in thorough mixing of air and, hence, uniform temperature distribution within the attic. The averaged Nusselt number for the hot ceiling wall which depicts the rate of convective heat transfer into the attic is in negative-gradient quasilinear relationship with the roof pitch. The practical significance of the predicted results is that, due to the peculiarity of the flat-top roof structure, heat loss to the attic is minimised when the roof pitch is relatively high; particularly not less than 300 and made as low as possible if the attic is to be used for drying of food crops.*

Keywords: *Flat-top, triangular, roofs, heated below, pitch angle, heat transfer*

Nomenclature

AR	*Aspect ratio*
G	*Gravitational acceleration, m/s²*
h	*Heat transfer coefficient, W/m²K*
H	*Height of enclosure, m*
k	*Thermal conductivity, W/m K*
L	*Length of enclosure, m*
Nu	*Nusselt number*
p	*Pressure*
Pr	*Prandtl number*
Ra	*Rayleigh number*
T	*Temperature, K*
Th	*Temperature at the hot wall, K*
Tc	*Temperature at the cold wall, K*
u	*Velocity in x-axis, m/s*
v	*Velocity in y-axis, m/s*
x, y	*Cartesian coordinates, m*

Greek letters

α	*Thermal diffusivity, m²/s*
β	*Coefficient of thermal expansion,0K*
θ	*Dimensionless temperature*
ν	*Kinematic viscosity, m²/s*
ρ	*Density, kg/m³*
ϕ	*Pitch angle, degrees*

subscripts

h	*hot wall*
c	*cold wall*

1. Introduction

In most residential, commercial and industrial buildings, the thermal characteristics of the attic space have significant influence on the cooling or heating load of the space directly below it. Therefore, for effective energy management, the roof attic is designed based on the heat transfer principles. For instance, in rural areas in Sub-Saharan Africa, agricultural produce are stored in the attics for accelerated drying. To obtain the expected uniform drying of these produce, it is imperative to have knowledge of the actual temperature distribution and the flow field in the attic which is influenced by the roof frame configuration. Over the years, temperature distribution and flow field within the attic and natural convective heat transfer across the ceiling have been subjects of investigation, more importantly, with the advent of unconventional roof designs.

The development of robust computational fluid dynamics (CFD) packages has made using them to obtain near-accurate numerical solutions of natural convection in enclosure problems. Comprehensive review on natural convective heat transfer across triangular enclosures carried out by Kamiyo et al. (2010) revealed extensive studies on regular pitched roofs and some complex-shaped roofs such as gambrel, gable and trapezoidal. Thereafter, investigations on heat transfer within attics of regular and complex shapes under different boundary conditions have continued.

Using two-dimensional (2D) unsteady CFD model, the impacts of roof pitch and ceiling insulation on the cooling load of gable-roof residential buildings were investigated by Wang et al. (2012) for attic spaces with roof pitches from 3/12 (14°) to 18/12 (60°) combined with ceiling insulation levels from R-1.2 to R-40. The results show that an increase of roof pitch from 3/12 to 8/12 results in a decrease in the cooling load by about 9%. The team further considered the effects of roof pitch on airflow and heating load of both sealed and vented attics for the same buildings in Wang and Shen (2012) and reported that airflow pattern in the sealed attics is steady and asymmetric, while that of the vented attics is a combination of symmetric base flow and a periodical oscillating flow.

Kamiyo et al. (2014) reported the flow structure and temperature distribution in asymmetric triangular enclosures heated from below in which they analysed the effects of the Rayleigh number and the pitch angle. The natural convection flow in an isosceles triangular enclosure subject to non-uniform cooling from the inclined surfaces and uniform heating from the base is investigated numerically by Saha and Gu (2015). The numerical simulation is performed using a finite volume method for a range of aspect ratio $0.2 \leq AR \leq 1.0$ and Rayleigh number $5 \times 10^4 \leq Ra \leq 1 \times 10^6$.

Sieres et al. (2016) reported an analytical and numerical computation of laminar natural convection in vertical upright–angled triangular cavities filled with air for angles 15°, 30°, 45° and Rayleigh number range: $0 \leq Ra < 10^9$. The vertical wall is heated with a uniform heat flux, the inclined wall is cooled at a uniform temperature while the upper horizontal wall is thermally insulated. At low Ra, heat transfer rate increases for lower angles but remains the same for high Ra. In a CFD modeling of a right-angled triangular enclosure, Mirabedin (2016) formulated a correlation for Nusselt number in terms of its aspect ratio and Rayleigh number and found that the Nusselt number increased with increase in aspect ratio.

In recent times, Amrani et al. (2017) numerically studied natural convection with surface radiation in a gabel roof for hot climates. Also, using 3D numerical model approach, Cui et al. (2019) carried out transient free convection heat transfer in a section-triangular prismatic enclosure with different aspect ratios and Ra range from 10^0 to 10^7 under top-cooled and bottom-heated boundary conditions to determine the critical Rayleigh numbers for the transition of the flow.

Archival literature has shown that knowledge of airflow and thermal characteristics of attic space is important and that knowledge could reliably be obtained using numerical simulation techniques. Many complex roof shapes have been studied but there are still some common ones that investigations have not covered sufficiently. The flat-top attic configuration shown in Figure 1 is one of such. In this study, a finite-volume CFD package is employed to better understand the steady airflow and temperature fields, and natural convective heat transfer into the attic of a flat-top roof heated through the ceiling.

Figure 1. Atypical Flat-top Roof House

2. Methods

Simply, the physical geometry of the attic of a pitched roof could be represented by a 2D triangular shape provided the roof extension in the direction perpendicular to the cross-section is more than double its width (Penot and N'Dame, 1992). Therefore, the physical geometry of the flat-top roof considered in this study, which coincides as the computational domain, is as shown in Figure 2. The horizontally truncated triangular structure of the geometry makes it appear like a low aspect ratio rectangle with inclined vertical sides. This peculiar shape is expected to affect the thermal performance of the roof in comparison with conventional roof shapes.

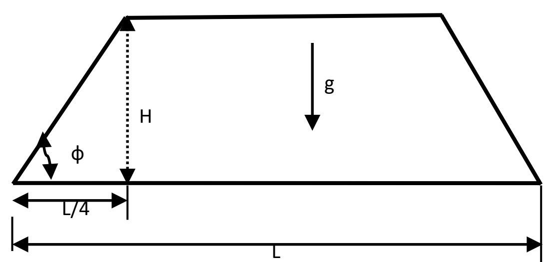

Figure 2. Computational Domain

The enclosure is filled with air. The base wall is heated isothermally; assuming the conventional hearth-heating method. The upper cold inclined and the flat-top walls (assumed made of aluminum) are set at a temperature difference of 20K with that of the hot ceiling (assumed made of gypsum board). There is no internal generation of heat. Being insignificant, the effect of the heat stored by the roof frame is neglected. The flow is assumed steady. Bousinessq approximation is applied;

the validity of which is corroborated by Gray and Giorgini (1976) and Ridouane et al. (2005). Actual roof size and real life weather conditions vary, hence, the domain dimensions and boundary conditions are normalised.

The governing equations for buoyancy-driven, laminar natural convective flow under steady-state conditions are conservation of mass, momentum and energy, expressed in dimensionless forms, subject to Bousinessq approximation, as:

Mass:

$$\frac{\partial U}{\partial X}+\frac{\partial V}{\partial Y}=0 \quad (1)$$

X-momentum:

$$U\frac{\partial U}{\partial X}+V\frac{\partial U}{\partial Y}=-\frac{\partial P}{\partial X}+\Pr\left(\frac{\partial^2 U}{\partial X^2}+\frac{\partial^2 U}{\partial Y^2}\right) \quad (2)$$

Y-momentum:

$$U\frac{\partial V}{\partial X}+V\frac{\partial V}{\partial Y}=-\frac{\partial P}{\partial Y}+\Pr\left(\frac{\partial^2 V}{\partial X^2}+\frac{\partial^2 V}{\partial Y^2}\right)+RaPr\theta \quad (3)$$

Energy:

$$U\frac{\partial \theta}{\partial X}+V\frac{\partial \theta}{\partial Y}=\left(\frac{\partial^2 \theta}{\partial X^2}+\frac{\partial^2 \theta}{\partial Y^2}\right) \quad (4)$$

Using the following non-dimensional variables:

$$X=\frac{x}{H},\ Y=\frac{y}{H},\ U=\frac{uH}{\alpha},\ V=\frac{vH}{\alpha},\ \theta=\frac{T-T_c}{T_h-T_c},$$

$$P=\frac{pH^2}{\rho\alpha^2},\ Pr=\frac{\nu}{\alpha} .$$

$$Ra=\frac{g\beta(T_h-T_c)H^3}{\alpha\nu}$$

Boundary Conditions:

Temperature: $\theta_c = 0$; $\theta_h = 1$

(isothermal roof and ceiling walls respectively)

Velocity: U = V = 0

(no-slip condition along the walls)

Four pitch angles, selected arbitrarily within the standard roof pitch range, are considered in the study. Computational parameters are as indicated in Table 1, indicating that the study is restricted to steady, laminar flow conditions.

Table 1: Computational Parameters

Pitch Angle (ϕ)	14^0	18^0	30^0	45^0
Aspect Ratio, AR = 4H/L	0.250	0.325	0.580	1.00
Rayleigh Number (Ra)	3.98 x10^4	8.75 x 10^4	4.97 x 10^5	2.55 x 10^6

The governing partial differential equations, with the associated buoyancy quantities, were discretized and solved using ANSYS FLUENT© (V18), a finite volume CFD package. SIMPLE algorithm as applied in the code was employed for the pressure-velocity coupling alongside a QUICK scheme adopted for spatial discretization of the momentum and energy equations. Convergence criteria were fixed at 10^{-5} for the continuity residual, and at 10^{-7} for the residuals of the momentum and energy equations. No slip condition was employed for velocity at the walls.

A combination of uniform and non-uniform meshes arrangement is implemented to capture the rapid changes in the dependent variables. To test grid independence of the solution scheme, many numerical runs were performed and the result of the Nusselt number variation for the 45º -pitch enclosure (see Figure 3) is as shown in Table 2.

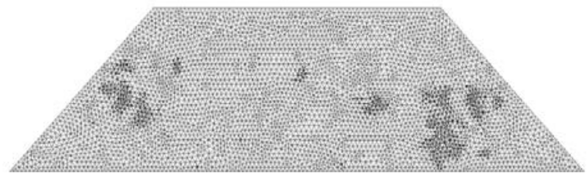

Figure 3. Computational Grid for the 45^0 Pitch Enclosure

Table 2. Grid Independence Study for the 45^0 Pitch Enclosure

Number of elements	41,113	46,921	50,744	54,536
Mean Nusselt number	17.736	19.134	19.665	19.710

Converged results show that the mesh with 50,000 elements was sufficient to produce grid independence.

3. Results and Discussion

The results of the simulations are presented in forms of predicted steady streamlines, velocity and temperature distributions within the attic alongside the local and averaged Nusselt number variations along the hot wall for the roof pitches considered. The velocity and temperature are scaled using $U=\sqrt{g\beta(T_h-T_c)H}$ and $\theta = (T - T_c)/(T_h - T_c)$ respectively; hence, range from zero to one.

3.1 Flow Field Analysis

The predicted streamlines in Figure 4 generally show that hot air rising from the hot, horizontal base wall hits the upper walls almost perpendicularly, then divides in either directions and returns to the base wall, thereby forming counter-rotating, recirculating cells. The flattop nature of the enclosure has peculiar influence on this flow structure. The closeness of the top and bottom walls constrained the cells to the lower part of the truncated triangle in a form similar to a low-height rectangular enclosure resulting in the classical Rayleigh-Bernard convection. In a regular triangular enclosure with the upper vertex, there are upper rows of cells formed as the pitch angle and Ra increase (Kamiyo et al., 2014). However, in the present study, the truncated nature of the enclosure prevents the formation of such upper cells.

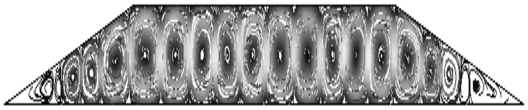

(a) 14°

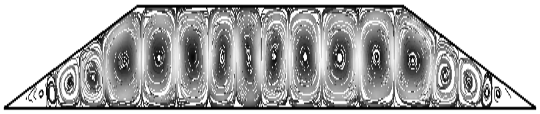

(b) 18°

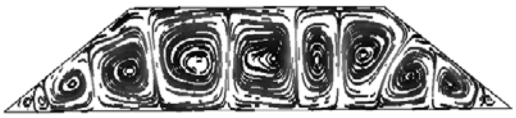

(c) 30°

(d) 45°

Figure 4. Streamlines for Different Pitch Angles

As the attic aspect ratio increases, the location of the counter-rotating vortices changes and their number also decreases. The strength of the vortices decreases with increase in pitch angle and from the midsection towards the bottom corners. This is due to the reducing effect of heat from the base wall (which is the same for all angles) as the pitch increases.

In the 14^o-pitch enclosure, Figure 4(a), there are twenty counter-rotating cells moving with different levels of intensity. While the size and the strength of the vortices under the flattop are relatively the same, those under the inclined walls naturally reduce in size towards the bottom corners. The strength of each cell reduces from the outer circumference towards the core; setting up regions of highest intensity where adjacent cells rub on each other. Near the intersections of the hot and cold walls, a very small region dominated by pure conduction exists. As the roof pitch increased to 18^o, Figure 4(b), thereby creating more space height to roam, the cells becomes larger and their number reduced to eighteen.

However, in Figure 4(c) for the 30^o-pitch, with almost double increase in the pitch angle, the central cells in the 18^o-pitch cavity merged to form larger cells. Also, the conduction region has become smaller. In the 45^o pitch cavity, Figure 4(d), there are just four counter-rotating cells as two cells in the 30^o-pitch enclosure appeared to have merged to form one. The formation of the vortices depends largely on the Rayleigh number, which at the same temperature difference and length of base wall, depends solely on the characteristic length, H which increases with the pitch angle.

Counter-rotating vortices obtained in this study is similar to that reported by Holtzman et al. (2000) who presented flow visualisation results from experiments performed in a smoke-filled isosceles triangular enclosure heated from the base wall, to show that, as Ra increases for a given geometry, the flow pattern becomes multi-cellular and the number of counter-rotating cells increases.

Figure 5 gives the variation of the predicted velocity at the mid height (Y= 0.5H) of the attic for different roof pitches. The velocity value has peaks at the point where adjacent cells rub on each other and low values at the core of the cells. The distance between two peaks therefore corresponds to the diameter of a cell.

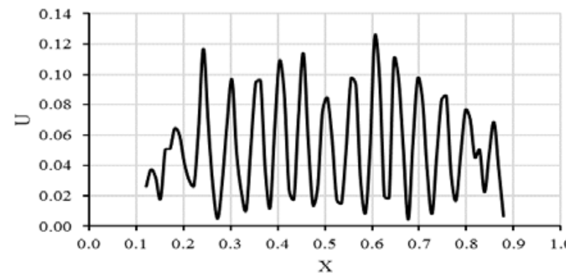

(a) 14°

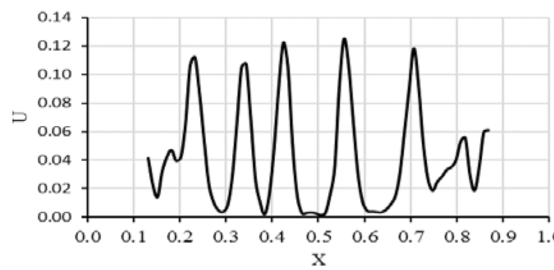

(b) 18°

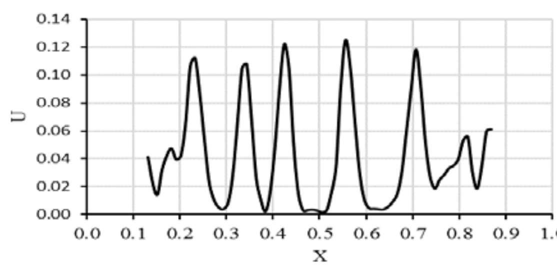

(c) 30°

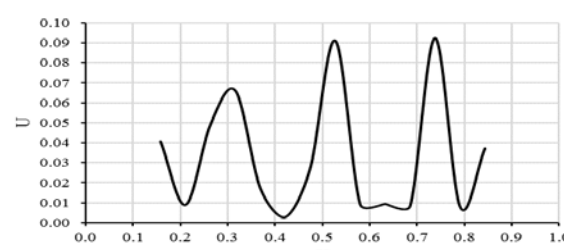

(d) 45°

Figure 5. Velocity Variations at Mid height (Y= 0.5H) for Different Roof Pitches

Velocity value is relatively high in major part of the cavities with an average value of about U = 0.06 but low in the 450-pitch where it is 0.045. The latter is due to low heating effect of the base wall on the cold volume of air within the cavity. Velocity variation plot at a cross-section in the enclosure is useful for predicting the convection currents that could guide in the proper ventilation of the attic space and on the best arrangement of food crops for uniform drying.

The air velocity profiles at the centerline (X = 0.5L) for different roof pitches are presented in Figure 6. It is observed that, in the 14° and 45° roof pitches, the centerline coincides with where two vortices at the midcentre rub on each other. The value of the air velocity increases gradually from the base wall as hot air rises and peaks at the midheight. It then gradually reduces to almost zero as the air dissipates most of its heat content to the cold flat-top wall. On the other hand, in the 18° and 30° pitches, the centerline coincides with the diameter of the midcentre cell rotating within the lower and upper boundary layers at $Y \leq 0.1$ and $Y \geq 0.9$ respectively. The air velocity value changed sharply within the boundary layers while its lowest value is at the core of the cells.

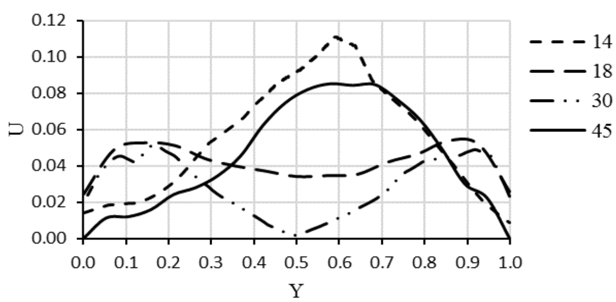

Figure 6. Velocity Profiles at Centre line (X = 0.5 L) for Different Roof Pitches

3.2 Temperature Distribution

The results of the predicted thermal field show domination by convection in all the roof pitch and Ra range considered. The predicted isotherm contours in Figure 7 indicate the presence of thermal plumes of hot air rising from the hot ceiling towards the cold roof walls and of cold jets leaving the cold roof walls downward. These correspond to regions between two counter-rotating vortices. Also, temperature gradient is very high at the thermal boundary layers along the walls. The strength and number of the vortices is observed to have strong influence on the transport processes within the enclosures. Analogous to the convection currents, the number of thermals progressively reduces as the roof pitch increases. Also, the isotherms in between the plumes become more spatial indicating reducing average temperature.

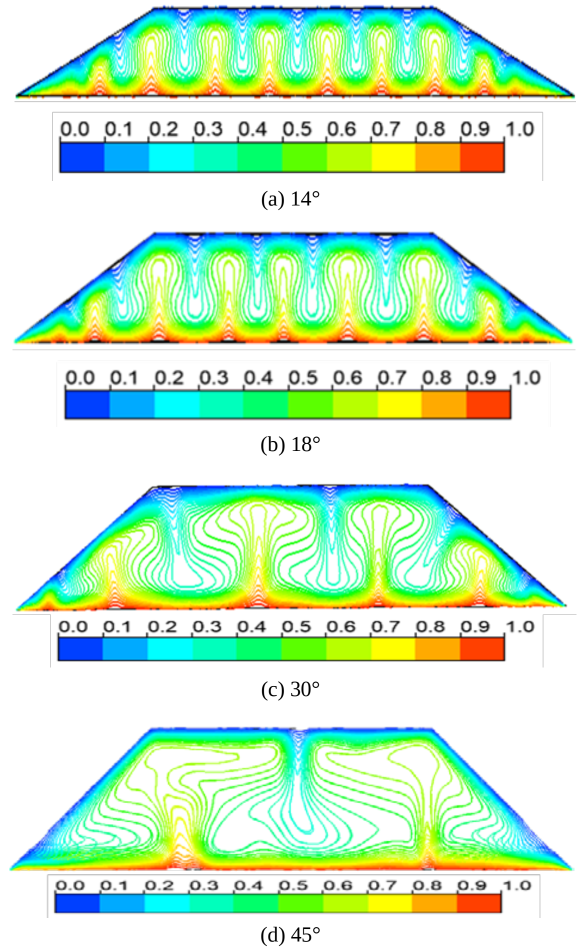

Figure 7. Isotherms for different roof pitches

What started as ten rising plumes in the 14°-pitch cavity, Figure 7(a), reduced drastically to two in the 45°-pitch in Figure 7(d). The multi-cellular flow within the 14°-pitch enclosure reported in Figure 4(a) results in a thorough mixing of the fluid to which corresponds a relatively high value of the mean temperature. Generally, the temperature distribution within an enclosure becomes progressively more uniform as the attic aspect ratio and the Rayleigh number increase. This effect is directly related to the formation of big vortices whose central part remains practically isothermal. Thermal boundary layers are formed along the hot and cold walls. The thickness of boundary layers increases with the roof pitch. At the bottom corners, heat transfer is very high due to the closeness of the hot and cold walls. It is suggested that insulation around that region of the ceiling should be reinforced to reduce heat loss into the attic while the locations are well suited for crop drying.

The variation of the predicted temperature at the midheight (Y = 0.5H) of the attic for different roof pitches is presented in dimensionless form in Figure 8. The peaks correspond to the centres of the hot plumes while the valleys are at the middle of the cold jets. The distance between two peaks gives the thickness of a cold jet while the thickness of a plume is determined by the distance between two valleys. The plot is useful to determine the location and degree of hotness of plumes which could guide in the arrangement of agricultural produce on the ceiling for proper drying.

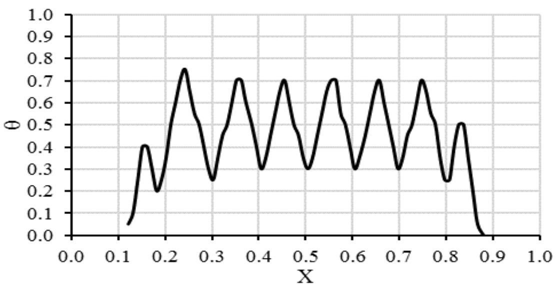

(a) 14°

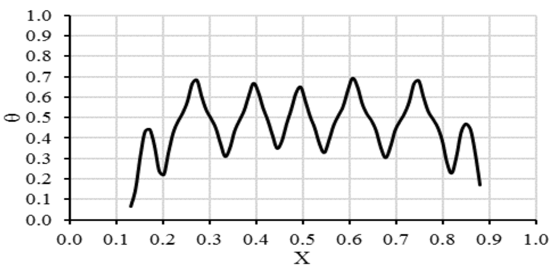

(b) 18°

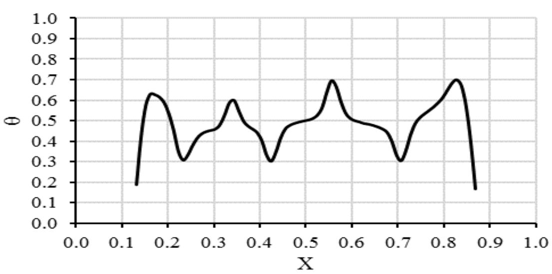

(c) 30°

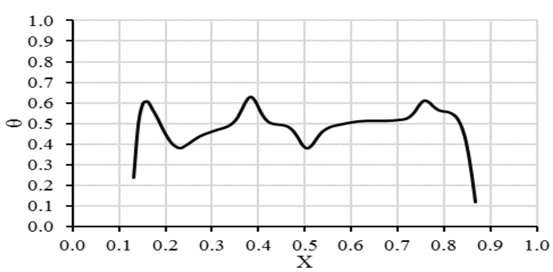

(d) 45°

Figure 8. Temperature Variation at Mid height (Y= 0.5H) for Different Roof Pitches

The temperature profiles at the centerline (X = 0.5L) of each roof pitch are presented in Figure 9(a). Generally, the profiles indicate two distinct regions: the lower and upper thermal boundary layers at Y ≤ 0.2 and Y ≥ 0.8, respectively, where air temperature drops sharply and a practically isothermal core. The predicted air temperature for the 30° roof pitch with Ra = 4.97 x10^5 is compared with a closely related experimental data of Flack (1980) at Ra = 4.5 x 10^5 in Figure 9(b). The agreement is good and adequate.

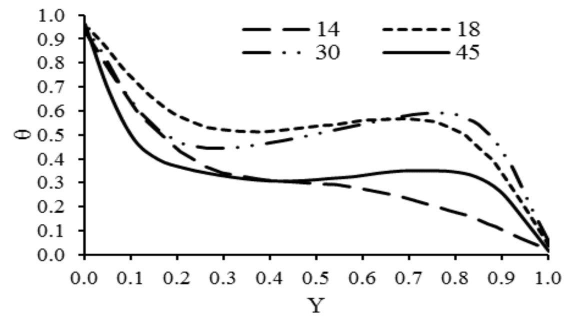

(a)

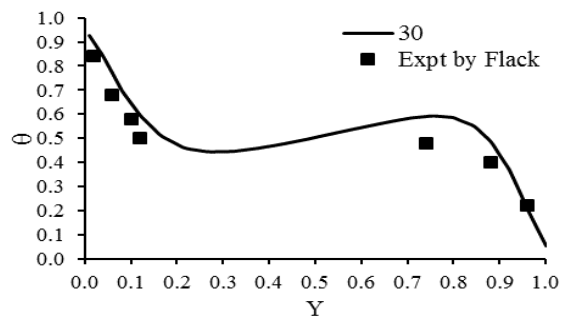

(b)

Figure 9. Temperature Profiles at the Centre line (X = 0.5L) for, (a) Different Roof Pitches, and (b) 30° Roof Pitch (Ra = 4.97 x10^5) and Flack Experiment (Ra = 4.5 x10^5)

3.3 Heat Transfer Analysis

The heat transfer pattern within the enclosures is reported with the plots of the values of the local Nusselt number along the walls and mean Nusselt number along the hot wall in Figures 10 and 11, respectively. In this study, the local Nusselt number is defined as:

$$Nu_x = \frac{h_x L}{k} \quad (5)$$

and, the mean Nusselt number as:

$$\overline{Nu} = \frac{\bar{h} L}{k} \quad (6)$$

where the ceiling length L, common to the enclosures, is chosen as the characteristic length.

The order of variation of the Nu_x along the hot ceiling and cold roof walls corroborate the fact that the rate of heat transfer from the walls synchronizes with the pattern of attachment and detachment of the thermal plumes at the walls. Particularly, in Figure 10, the upper values in the local Nu plot for the 14°-pitch cavity directly correspond to thermal plume crash and separation points on the walls. The relatively sequential wavy Nu_x lines indicate uniform heat flow across the enclosure.

In the 45°-pitch, this is no longer the case. The trends become irregular and the relatively low values of Nu_x under the flattop wall show that heat transfer from the base wall, at that roof pitch, is quite low; the average temperature within the cavity tends towards that of the upper cold wall. Similar result was obtained by Haese and Teubner (2002). In all the roof pitches considered, high Nu-values are found in the vicinity of the bottom corners, mainly due to the closeness of the hot and cold walls. In solar drying in the tropics, the agricultural produce is contained in an enclosed space and the air in contact with it is heated by solar radiation. By heating the air, its capacity to attract moisture from the environment increases. Therefore, grains dry faster and better when placed in the high temperature region near the bottom corners.

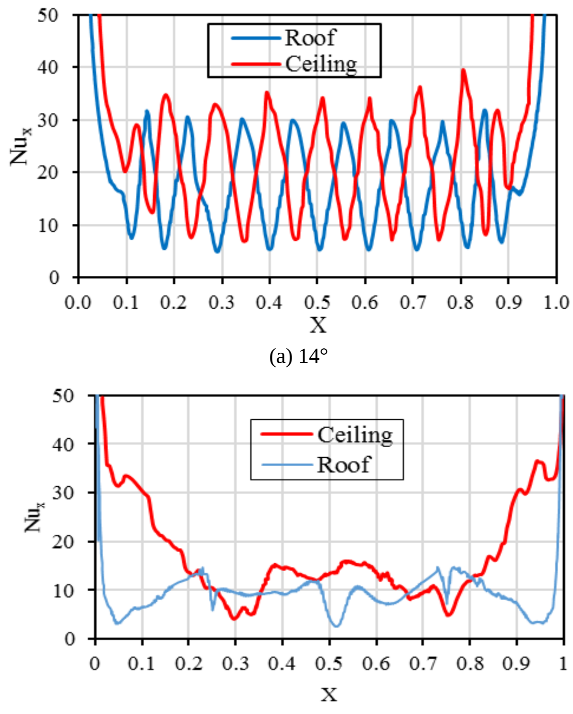

Figure 10. Variation of Local Nusselt Number along the Walls for (a) 14^0- and (b) 45^0- Pitch Enclosures

In order to predict the effect of pitch angle on the rate of heat loss from the heated space through the ceiling into the attic of a flat-top roof, the plot of values of the mean Nusselt number against roof pitch is presented in Figure 11. The plot shows that the $\overline{Nu}$ is in negative-gradient quasilinear relationship with the roof pitch. That is, the heat transfer rate reduces as the roof pitch increases; specifically $\overline{Nu}$ varies inversely with $\phi^{1/3}$.

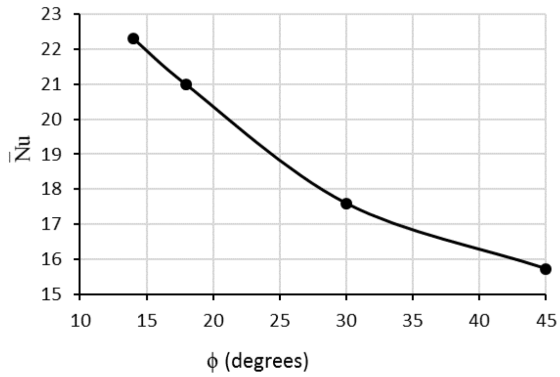

Figure 11. Variation of mean Nusselt number on the hot wall for different enclosures

In other words, the higher the roof pitch, the longer the length of the cold wall, the higher the distance between the hot and cold walls and the higher the volume of attic air to heat. Therefore, for the same length of the ceiling and same heating rate, the heating effect reduces. It is then concluded that due to the peculiarity of the flat-top roof structure, to minimise heat loss to the attic, the roof pitch should be relatively high; particularly not less than 30°. On the other hand, if the attic is to be used for effective drying of food crops, as in sub-Saharan rural villages, the roof pitch should be as low as possible.

4. Conclusion

The fluid dynamics and heat transfer of air within the attic of a flat-top roof structure at varying pitch angles has been predicted for bottom heating condition using numerical technique. The results show that the peculiar shape of the roof has significant effects on the fluid flow and heat transfer. Particularly, the truncated triangular architecture of the roof prevents the formation of upper-row counter rotating cells in the attic. Also, the number of the cells formed reduces as pitch angle (or aspect ratio) increases. At low roof pitch, the high intensity of the vortices causes uniform flow field and temperature distribution within the attic.

The averaged Nusselt number for the hot ceiling wall which depicts the rate of convective heat transfer into the attic is in negative-gradient quasilinear relationship with the roof pitch. For the range of pitch angle considered, the heat transfer rate is higher near the lower base corners than any part of the flow area. The practical significance of the predicted results is that, due to the peculiarity of the flat-top roof structure, heat loss to the attic is minimised when the roof pitch is relatively high; particularly not less than 30° and made as low as possible if the attic is to be used for drying of food crops.

This work will be useful to building designers in their choice of insulation material for controlling heat losses through flat top attic spaces. Also, knowledge of the flow pattern of the hot air within the attic enables agriculturalists in a tropical environment to predict the most appropriate positions for placing farm produce especially when the control of drying- and moisture-removal rates is important.

References:

Amrani A., Dihmani N., Amraqui S., and Mezrhab A. (2017), "Analysis of combined natural convection and thermal radiation heat transfer in a triangular shaped roof for hot climates", *Journal of Materials and Environmental Sciences*, Vol. 8, No., pp. 3013-3027.

Cui, H., Xu, F., Sahad, S., and Liu, Q. (2019), "Transient free convection heat transfer in a section-triangular prismatic enclosure with different aspect ratios", *International Journal of Thermal Sciences*, Vol. 139, pp.282-291.

Flack, R.D. (1980), "The experimental measurement of natural convection heat transfer in triangular enclosures heated or cooled from below", *Journal of Heat Transfer*, Vol.102, pp.770-772.

Gray, D.D., and Giorgini, A., (1976), "The validity of the Boussinesq approximation for liquids and gases", *International Journal of Heat and Mass Transfer*, Vol. 19, pp.545-551.

Haese, P.M., and Teubner, M.D. (2002), "Heat exchange in an attic space", *International Journal of Heat and Mass Transfer*, Vol. 45, pp.4925-4936.

Holtzman, G.A., Hill, R.W., and Ball, K.S. (2000), "Laminar natural convection in isosceles triangular enclosures heated from below and symmetrically cooled from above", *Journal of Heat Transfer*, Vol.122, No.3, pp.485-491.

Kamiyo, O.M., Angeli, D., Barozzi, G.S., and Collins, M.W. (2014), "Natural convection in asymmetric triangular enclosures heated from below", *Journal of Physics*, Vol.547, pp.1-10.

Kamiyo, O.M., Angeli, D., Barozzi, G.S., Collins, M.W., Olunloyo, V.O.S., and Talabi, S.O. (2010), "A comprehensive review of natural convection in triangular enclosures", *Journal of Applied Mechanics Review: Transactions of ASME*, Vol. 63, 060801, 13 pages.

Mirabedin, S., (2016), "CFD modelling of natural convection in right–angled triangular enclosures", *International Journal of Heat Technology*, Vol. 34, No.3, pp. 503-506.

Penot, F., and N'Dame, A. (1992), "Successive bifurcations of natural convection in a vertical enclosure heated from the side", *Heat Transfer: Proceedings of the 3rd UK National Conference and First European Conference on Thermal Sciences*, Birmingham, UK, Vol.1, pp.507-513.

Ridouane, E. H., Campo, A., and McGarry, M. (2005), "Numerical computation of buoyant airflows confined to attic spaces under opposing hot and cold wall conditions", *International Journal of Thermal Sciences*, Vol. 44, pp. 944-952.

Saha, S.C., and Gu, Y.T. (2015), "Natural convection in a triangular enclosure heated from below and non-uniformly cooled from top", *International Journal of Heat and Mass Transfer*, Vol.80, pp.529-538.

Sieres, J., Campo, A., and Martinez-Suarez, J.A. (2016), "Natural convection air flow in vertical upright–angled triangular cavities under realistic thermal boundary conditions", *Journal of Thermal Science*, Vol.20, No.5, pp.1407-1420.

Wang, S., and Shen, Z. (2012), "Effects of roof pitch on air flow and heating load of sealed and vented attics for gable-roof residential buildings", *Sustainability*, Vol.4, No.9, pp.1999-2021.

Wang, S., Shen, Z., and Gu, L. (2012), "The impact of roof pitch and ceiling insulation on cooling load of naturally-ventilated attics", *Energies*, Vol. 5, No.7, pp.2178-2196.

Author's Biographical Notes:

Ola Kamiyo *is a Senior Lecturer and immediate past Head of the Department of Mechanical Engineering, University of Lagos, Lagos, Nigeria where he is actively involved in both teaching and research at the postgraduate level. Dr. Kamiyo holds a BSc, MSc and PhD degrees in Mechanical Engineering at the Department of Mechanical Engineering, University of Lagos. He was a visiting Research Fellow at the Department of Engineering "Enzo Ferrari", University of Modena and Reggio Emilia, Modena, Italy. His areas of research interest include heat transfer in enclosures and thermal properties of novel building materials.*

■